1521-009X/45/3/279–285$25.00
Drug Metabolism and Disposition

http://dx.doi.org/10.1124/dmd.116.073494
Drug Metab Dispos 45:279–285, March 2017

Functional Characterization of 34 CYP2A6 Allelic Variants by Assessment of Nicotine *C*-Oxidation and Coumarin 7-Hydroxylation Activities

Hiroki Hosono, Masaki Kumondai, Masamitsu Maekawa, Hiroaki Yamaguchi, Nariyasu Mano, Akifumi Oda, Noriyasu Hirasawa, and Masahiro Hiratsuka

Laboratory of Pharmacotherapy of Life-Style Related Diseases, Graduate School of Pharmaceutical Sciences, Tohoku University, Sendai, Japan (H.H., M.K., N.H., M.H.), Department of Pharmaceutical Sciences, Tohoku University Hospital, Sendai, Japan (M.M., H.Y., N.M.), Department of Biophysical Chemistry, Faculty of Pharmacy, Meijo University, Nagoya, Japan (A.O.)

Received September 7, 2016; accepted December 13, 2016

ABSTRACT

CYP2A6, a member of the cytochrome P450 (P450) family, is one of the enzymes responsible for the metabolism of therapeutic drugs and such tobacco components as nicotine, 4-(methylnitrosamino)-1-(3-pyridyl)-1-butanone, and *N*-nitrosodiethylamine. Genetic polymorphisms in CYP2A6 are associated with individual variation in smoking behavior, drug toxicities, and the risk of developing several cancers. In this study, we conducted an in vitro analysis of 34 allelic variants of CYP2A6 using nicotine and coumarin as representative CYP2A6 substrates. These variant CYP2A6 proteins were heterologously expressed in 293FT cells, and their enzymatic activities were assessed on the basis of nicotine *C*-oxidation and coumarin 7-hydroxylation activities. Among the 34 CYP2A6 variants, CYP2A6.2, CYP2A6.5, CYP2A6.6, CYP2A6.10, CYP2A6.26, CYP2A6.36, and CYP2A6.37 exhibited no enzymatic activity, whereas 14 other variants exhibited markedly reduced activity toward both nicotine and coumarin. These comprehensive in vitro findings may provide useful insight into individual differences in smoking behavior, drug efficacy, and cancer susceptibility.

Introduction

CYP2A6, a member of the cytochrome P450 (P450) family, is the primary enzyme involved in the oxidative metabolism of nicotine and such clinically useful drugs as metronidazole, methoxyflurane, tegafur, valproic acid, and fadrozole (Kharasch et al., 1995; Nakajima et al., 1996; Sadeque et al., 1997; Komatsu et al., 2000; Pelkonen et al., 2000; Pearce et al., 2013). This enzyme also plays an important role in the metabolic activation of 4-(methylnitrosamino)-1-(3-pyridyl)-1-butanone (NNK) and *N*-nitrosodiethylamine (NNN), major constituents in tobacco smoke (Crespi et al., 1991). Nicotine, the main driver in the development and maintenance of tobacco dependence, is primarily metabolized to cotinine (70–80%) by CYP2A6 (Fig. 1) (Benowitz et al., 1995; Fagerström and Balfour, 2006). A phenotype study using nicotine as the CYP2A6 probe substrate discovered significant individual variability in CYP2A6 activity (Nakajima et al., 2006). A meta-analysis suggested that reduced metabolizers (patients with low CYP2A6 activity) smoke fewer cigarettes per day than normal metabolizers (Pan et al., 2015). The presence of several *CYP2A6* variants explains why large deviation fractions were observed in estimated nicotine biomarker metabolism rates that were identified in a genome-wide association study (Loukola et al., 2015). Furthermore, CYP2A6 activity was significantly correlated not only with increased nicotine uptake but also with the effect that causes smokers to smoke more extensively (Patel et al., 2016). Tegafur, a prodrug of 5-fluorouracil (5-FU), is another clinically important CYP2A6 substrate in human liver microsomes (Yamamiya et al., 2014). CYP2A6 enzymatic activity variation would affect the therapeutic effect through 5-FU biokinetics.

Investigating the enzymatic functions of individual CYP2A6 allelic variants in vivo is difficult because the number of patients carrying low-frequency alleles is limited (Soriano et al., 2011). Therefore, in vitro characterization of CYP2A6 variant activity using a recombinant enzyme system is essential for a deeper understanding of the individual variability in drug response and toxicity. Various heterologous expression systems, including bacteria, yeast, insect cells, and mammalian cells, have been used in previous studies (Hiratsuka, 2012). Through the use of these systems, several CYP2A6 variants have been found to exhibit reduced catalytic activities toward various CYP2A6 substrates compared with those of the wild type, CYP2A6.1 (Kitagawa et al., 2001; Daigo et al., 2002; Han et al., 2012; Yamamiya et al., 2014). However, these studies assessed different kinetic parameters [Michaelis constant (K_m), maximum velocity (V_{max}), and intrinsic clearance (CL_{int})]. In addition, post-translational processing of proteins expressed in bacteria, yeast, and baculoviruses differs from that in mammalian cells (Oldham, 1998; Hiratsuka, 2012). Such differences in expression systems may result in discrepancies in findings and conclusions.

This study was supported in part by a grant from the Ministry of Health, Labour and Welfare (MHLW) of Japan ("Initiative to facilitate development of innovative drug, medical devices, and cellular and tissue-based product"), the Smoking Research Foundation, and the Japan Research Foundation for Clinical Pharmacology.

H.H. and M.K. contributed equally to this work.

dx.doi.org/10.1124/dmd.116.073494.

ABBREVIATIONS: CL_{int}, intrinsic clearance; G-6-P, glucose-6-phosphate; G-6-PDH, glucose-6-phosphate dehydrogenase; UHPLC, ultra-high-performance liquid chromatography; K_m, Michaelis constant; LC-MS/MS, liquid chromatography–tandem mass spectrometry; NNK, 4-methylnitrosoamino-1-(3-pyridyl)-1-butanone; NNN, *N*-nitrosodiethylamine; P450, cytochrome P450; SRS, substrate-recognition site; 3D, three-dimensional; V_{max}, maximum velocity.

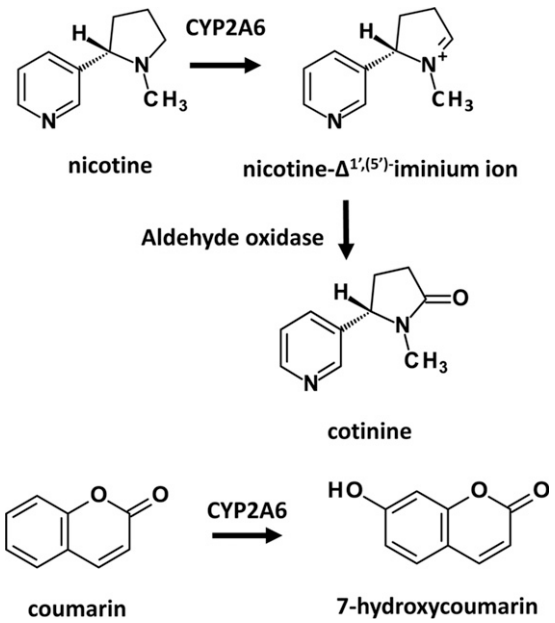

Fig. 1. Metabolic pathways for nicotine showing the first reaction, catalyzed by CYP2A6, and the second reaction, catalyzed by aldehyde oxidase (upper). Primary metabolic pathway of coumarin (lower).

A large number of genetic polymorphisms in the *CYP2A6* gene have been identified in several ethnic groups and shown to contribute to altered enzyme activation and expression (Fernandez-Salguero et al., 1995; Oscarson et al., 1999; Kiyotani et al., 2002; Haberl et al., 2005; Al Koudsi et al., 2009; Piliguian et al., 2014). These polymorphisms are thought to produce individual variations in pharmacokinetics, drug efficacy, adverse drug reactions, and drug toxicities (Fujieda et al., 2004; Wang et al., 2011; Yamamiya et al., 2014; Hosono et al., 2015; Kumondai et al., 2016). To date, 45 CYP2A6 allelic variants have been identified [http://www.cypalleles.ki.se/cyp2a6.htm (accessed September 5, 2016)]. Although most of these alleles carry amino acid substitutions, *CYP2A6*3, CYP2A6*4, CYP2A6*12, CYP2A6*20, CYP2A6*27,* and *CYP2A6*34* are known to be inactive as a result of frame-shift mutations, gene conversion with the pseudogene *CYP2A7* (another member of the human P450 subfamily), or whole-gene deletion. *CYP2A6*9* is reported to exhibit reduced transcriptional activity owing to a point mutation in the TATA box, located in the 5′ flanking region. Information regarding *CYP2A6*29, CYP2A6*30, CYP2A6*32,* and *CYP2A6*33* is currently unavailable. After removal of the above mentioned alleles, 34 CYP2A6 variants remained for characterization. To characterize these 34 CYP2A6 variants, we assessed their functional activities over a nicotine substrate following protein expression in 293FT cells. Additionally, coumarin was used as another substrate for CYP2A6 to determine whether the observed functional changes were substrate-dependent (Miles et al., 1990).

Materials and Methods

Chemicals. (–)-Nicotine, (–)-cotinine, and (±)-cotinine-(methyl-d3) derivatives, as well as coumarin, 7-hydroxycoumarin, and 4-methyl-7-hydroxycoumarin were purchased from Sigma-Aldrich (Tokyo, Japan). CYP2A6 baculosomes and Ultrapool Human Liver Cytosol, 150-Donor Pool, were purchased from Corning Incorporated (Corning, NY). $NADP^+$, glucose-6-phosphate (G-6-P), and glucose-6-phosphate dehydrogenase (G-6-PDH) were purchased from Oriental Yeast (Tokyo, Japan). The polyclonal anti-human CYP2A6 antibody was purchased from Nosan Corporation (Kanagawa, Japan). The polyclonal anti-calnexin antibody was purchased from Enzo Life Sciences (Farmingdale, NY). Horseradish peroxidase-conjugated goat anti-rabbit IgG was purchased from Santa Cruz Biotechnology (Dallas, TX).

***CYP2A6* cDNA Cloning and Construction of Expression Vectors.** *CYP2A6* cDNA fragments, obtained from a human liver cDNA library (Takara, Shiga, Japan) , were amplified by polymerase chain reaction with a forward primer (5′-CACCATGCTGGCCTCAGGGATGCTTC-3′) and reverse primer (5′-TCAGCGGGGCAGGAAGCTCATGGTGTAG-3′) using PfuUltra High-Fidelity DNA Polymerase (Agilent Technologies, Santa Clara, CA). The underlined sequences in the forward primer were introduced for directional TOPO cloning. The amplified fragments were subcloned into the pENTR/D-TOPO vector (ThermoFisher Scientific, Waltham, MA). Plasmids carrying *CYP2A6*1* cDNA (wild-type) were used as a template to generate various *CYP2A6* constructs (*CYP2A6*2, CYP2A6*5–CYP2A6*8, CYP2A6*11, CYP2A6*13–CYP2A6*18, CYP2A6*21–CYP2A6*23, CYP2A6*25, CYP2A6*28, CYP2A6*31, CYP2A6*35, CYP2A6*38–CYP2A6*43,* and *CYP2A6*45*) using a QuikChange Lightning Site-Directed Mutagenesis Kit (Agilent Technologies) according to the manufacturer's instructions. Other *CYP2A6* constructs were generated from plasmids carrying other cDNA templates: *CYP2A6*10, CYP2A6*19,* and *CYP2A6*36* from *CYP2A6*7* cDNA; *CYP2A6*24* from *CYP2A6*35* cDNA; *CYP2A6*26* from *CYP2A6*25* cDNA; *CYP2A6*37* from *CYP2A6*10* cDNA; and *CYP2A6*44* from *CYP2A6*28* cDNA. All prepared constructs were confirmed by direct sequencing. The wild-type and variant *CYP2A6* cDNA sequences were subsequently subcloned into the mammalian expression vector pcDNA3.4 (ThermoFisher Scientific).

Expression of CYP2A6 Variant Proteins in 293FT Cells. We cultured 293FT cells in Dulbecco's modified Eagle's medium (Nacalai Tesque, Kyoto, Japan) containing 10% fetal bovine serum at 37°C in the presence of 5% CO_2. Cells were transfected with plasmid (5 μg) carrying *CYP2A6* cDNA using TransFectin Lipid Reagent (Bio-Rad Laboratories, Hercules, CA), according to the manufacturer's instructions. After incubation for 24 hours at 37°C, cells were scraped off, centrifuged at 1500*g* for 5 minutes, and resuspended in homogenization buffer [10 mM Tris-HCl (pH 7.4), 1 mM EDTA, and 10% glycerol]. Microsomal fractions were prepared by differential centrifugation at 9000*g* for 20 minutes, followed by centrifugation of the resulting supernatant at 105,000*g* for 60 minutes. The microsomal pellet was resuspended in 50 mM Tris-HCl (pH 7.4) containing 1 mM EDTA, 20% glycerol, 150 mM KCl, and Protease Inhibitor Cocktail for Use with Mammalian Cell and Tissue Extract (Nacalai Tesque) and stored at –80°C. The protein concentration was determined using a BCA Protein Assay Kit (ThermoFisher Scientific).

Determination of Protein Expression Levels by Immunoblotting. We separated 293FT microsomal fractions (4 μg of microsomal protein) by electrophoresis on 10% SDS-polyacrylamide gels. Western blotting was performed in triplicate for each CYP2A6 variant protein in accordance with standard procedures. Recombinant CYP2A6 supersome was used as the standard (0.06–0.50 pmol) in each gel to quantify the CYP2A6 protein level. CYP2A6 protein was detected using a polyclonal anti-human CYP2A6 antibody (diluted at 1:10,000), and calnexin, used as a loading control, was detected using a polyclonal anti-calnexin antibody (diluted at 1:5000). Secondary detection was carried out with horseradish peroxidase-conjugated goat anti-rabbit IgG (diluted at 1:10,000). Immunoblots were visualized using SuperSignal West Pico Chemiluminescent Substrate (ThermoFisher Scientific). Chemiluminescence was quantified using a ChemiDoc XRS^+ with the help of Image Laboratory Software (Bio-Rad Laboratories).

Nicotine *C*-Oxidation Assay. Nicotine *C*-oxidation by CYP2A6 was measured as reported previously (Nakajima et al., 1996) with several modifications. The incubation mixture consisted of the microsomal fraction (20 μg), Ultrapool Human Liver Cytosol, 150-Donor Pool, as a source of aldehyde oxidase (10 μg), nicotine (10, 25, 50, 100, 250, 500, or 1000 μM), and 50 mM potassium phosphate buffer (pH 7.4) in a total volume of 100 μl. Following preincubation at 37°C for 3 minutes, reactions were initiated by addition of NADPH-generating medium, consisting of 0.5 mM $NADP^+$, 5 mM G-6-P, 5 mM MgCl, and 1 IU/ml G-6-PDH. The mixture was incubated at 37°C for 20 minutes. Reactions were terminated by adding 100 μl of acetonitrile containing 1 μM of cotinine-(methyl-d3) (internal standard). Measurement of nicotine *C*-oxidation using 100 μM of nicotine and 20 μg of microsomal fraction containing the wild-type and variant CYP2A6 showed that cotinine formation was linear for incubations of up to 20 minutes. Moreover, when the reaction containing 100 μM nicotine was

incubated for 20 minutes, cotinine formation was linear in the presence of up to 20 μg of microsomal protein (data not shown).

After protein removal by centrifugation at 15,400*g* for 10 minutes, the supernatant was diluted twice with water, and 10 μl of diluted solution was injected into a liquid chromatography–tandem mass spectrometry (LC-MS/MS) system. Cotinine was measured using the LC-MS/MS system in the positive ion detection mode at the electrospray ionization interface (TSQ Vantage Triple Stage Quadrupole Mass Spectrometer; ThermoFisher Scientific). Separation by ultra-high-performance liquid chromatography (UHPLC) was conducted using the Nexera Ultra High Performance Liquid Chromatograph system (Shimadzu, Kyoto, Japan). Chromatographic separation was performed using a CAPCELL PAK ADME S2 (2.1 × 50 mm, 2.0-μm particle size; Shiseido, Tokyo, Japan) maintained at 35°C. Cotinine was eluted isocratically with a mobile phase consisting of 0.05% (v/v) formic acid in water and 0.05% (v/v) formic acid in acetonitrile (90:10, v/v) at a flow rate of 200 μl/min.

Quantitative MS/MS analyses were performed in the selective reaction monitoring mode. The area under the peak of *m/z* 177 → 80 (collision energy, 24 V; S-Lens RF amplitude voltage, 85 V) for cotinine and of *m/z* 180 → 80 (collision energy, 29 V; S-Lens RF amplitude voltage, 55 V) for cotinine-(methyl-d3) was measured. The optimized parameters for MS were as follows: spray voltage, 4.5 kV; sheath gas pressure, 60 psi; vaporizer temperature, 200°C; capillary temperature, 205°C; and collision pressure, 1.7 mTorr. The sheath gas was nitrogen, and the collision gas was argon. The LC-MS/MS system was controlled by Xcalibur software (ThermoFisher Scientific), which was also used to analyze the data. The lower limit of cotinine quantification was 10 nM. Standard curves for cotinine were constructed in the 0.01–30 μM range using authentic metabolite standards. The enzymatic activity was normalized to the corresponding CYP2A6 expression level.

Coumarin 7-Hydroxylation Assay. The coumarin 7-hydroxylation activity of CYP2A6 was determined using previously reported methods (Ho et al., 2008) with minor modifications. The reaction mixture contained the microsomal fraction (30 μg), coumarin (0.1, 0.25, 0.5, 1.0, 2.5, 5.0, 10, or 25 μM), and 50 mM potassium phosphate buffer (pH 7.4) in a total volume of 100 μl. Following preincubation at 37°C for 3 minutes, reactions were initiated by the addition of NADPH-generating medium (see above). The mixture was incubated for an additional 10 minutes at 37°C. Reactions were terminated by adding 100 μl of acetonitrile containing 250 nM of 4-methyl-7-hydroxycoumarin (internal standard). Determination of coumarin 7-hydroxylation activity in the microsomal fraction containing CYP2A6.1 (30 μg of microsomal protein) and 2.5 μM of coumarin revealed that 7-hydroxycoumarin formation was linear for incubations of up to 10 minutes. When the reaction containing 2.5 μM of coumarin was incubated for 10 minutes, 7-hydroxycoumarin formation was linear in the presence of up to 30 μg of microsomal protein (data not shown).

After protein removal by centrifugation at 15,400*g* for 10 minutes, the supernatant was diluted twice with 50 mM potassium phosphate buffer (pH 7.4), and 50 μl of the diluted solution was subjected to HPLC. The HPLC system consisted of a Waters 2695 Separations Module, a Waters 2475 Multi λ Fluorescence Detector (Waters, Milford, MA), and a SunFire C18 column (4.6 × 150 mm, 5-μm particle size; Waters) maintained at 40°C. We eluted 7-hydroxycoumarin isocratically with 20 mM potassium phosphate buffer (pH 7.4) and acetonitrile (70:30, v/v) at a flow rate of 0.5 ml/min. The quantity of 7-hydroxycoumarin was measured at an excitation wavelength of 376 nm and emission wavelength of 454 nm. The lower limit of 7-hydroxycoumarin quantification was 25 nM. Standard curves for 7-hydroxycoumarin were constructed in the 25–2000 nM range using authentic metabolite. The enzymatic activity was normalized to the CYP2A6 expression level.

Data Analysis. The kinetic data were analyzed using the Enzyme Kinetics Module of SigmaPlot 12.5 (Systat Software, Inc., Chicago, IL), a curve-fitting program on the basis of nonlinear regression analysis. K_m, maximum velocity (V_{max}), and intrinsic clearance ($CL_{int} = V_{max}/K_m$) values were determined by using this software. V_{max} was calculated using the average CYP2A6 expression level values in triplicate. All values are expressed as the mean ± S.D. of experiments performed in triplicate. Statistical analyses of enzymatic activity and kinetic parameters were performed by analysis of variance using Dunnett's T3 test or the Kruskal-Wallis method (IBM SPSS Statistics Ver. 22; International Business Machines, Armonk, NY). The correlation between the CL_{int} ratios of nicotine *C*-oxidation and coumarin 7-hydroxylation among CYP2A6 variants was analyzed using weighted linear regression analysis (IBM SPSS Statistics). Differences or correlations with *P* values of less than 0.05 were defined as significant.

Three-Dimensional Structural Modeling of CYP2A6. Three-dimensional (3D) structural modeling of CYP2A6 and nicotine binding was constructed on the basis of the DeVore and Scott (2012) CYP2A6 X-ray structure (Protein Data Bank code 4EJJ), and 3D structural modeling of CYP2A6 and coumarin docking was constructed on the basis of the Yano et al. (2005) CYP2A6 X-ray structure (Protein Data Bank code 1Z10). Maestro 9.7.012 (Schrodinger, LLC, New York, NY) was used for 3D imaging of CYP2A6.

Results

Protein levels of CYP2A6 variants expressed in 293FT cells were measured by immunoblotting. Polyclonal CYP2A6 antibodies recognized all CYP2A6 variant proteins (Fig. 2). Only CYP2A6.13 exhibited a double band, the bands at both molecular weights were quantified. Expression levels for calnexin, an endoplasmic reticulum-resident protein, were virtually constant in the microsomes of transfected cells. CYP2A6 protein was not detected in cells transfected with empty vector (mock transfection).

The kinetic parameters of nicotine *C*-oxidation were determined for the wild type (CYP2A6.1) and 26 CYP2A6 variants (Table 1). K_m, V_{max}, and CL_{int} values for nicotine *C*-oxidation by CYP2A6.1 were 33.3 μM, 5.91 pmol · min^{-1} · $pmol^{-1}$ CYP2A6, and 176 nl · min^{-1} · $pmol^{-1}$ CYP2A6, respectively. The kinetic parameters of four variants (CYP2A6.2, CYP2A6.5, CYP2A6.6, and CYP2A6.26) could not be determined because no nicotine *C*-oxidation activity was detected. The kinetic parameters of three variants (CYP2A6.10, CYP2A6.36, and CYP2A6.37) could not be determined because the amount of product was at or below the lower quantification limit at low substrate concentrations. The K_m value of CYP2A6.38 (108 μM) was significantly higher than that of the wild type. V_{max} values of CYP2A6 allelic variants were not significantly lower than those of the wild-type CYP2A6. The CL_{int} value for CYP2A6.15 was 1.2 times higher than that of CYP2A6.1.

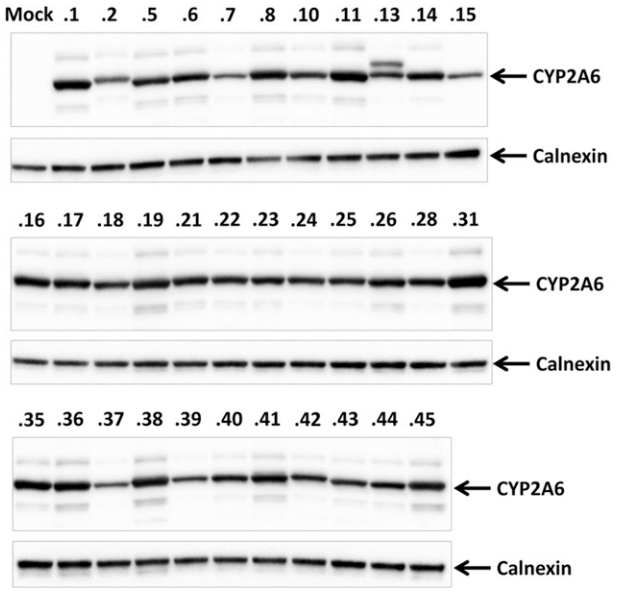

Fig. 2. Western blots showing immunoreactive CYP2A6 proteins (upper panel) and calnexin (lower panel). Microsomal protein fraction (4 μg) was loaded in each lane. Microsomal proteins were separated by electrophoresis on 10% SDS-polyacrylamide gels and then subjected to Western blotting according to standard procedures. The CYP2A6 variant proteins were detected using a polyclonal antibody against CYP2A6, and calnexin was detected using a polyclonal antibody against calnexin. Numbers correspond to CYP2A6 variants.

TABLE 1

Kinetic parameters of nicotine *C*-oxidation and coumarin 7-hydroxylation by microsomes from 293FT cells expressing CYP2A6 wild-type and variant proteins

These data represent the mean ± S.D. of three independently performed catalytic assays.

Variants	Nucleotide Changes	Amino Acid Changes	Nicotine *C*-Oxidation			Coumarin 7-Hydroxylation		
			K_m	V_{max}	CL_{int} (V_{max}/K_m)	K_m	V_{max}	CL_{int} (V_{max}/K_m)
			μM	*pmol/min per pmol CYP2A6*	*nl/min per pmol CYP2A6 (% of wild-type)*	*μM*	*pmol/min per pmol CYP2A6*	*μl/min per pmol CYP2A6 (% of wild-type)*
*CYP2A6*1*			33.3 ± 5.44	5.91 ± 1.26	176 ± 11.2	1.94 ± 0.06	5.89 ± 0.34	3.04 ± 0.08
*CYP2A6*2*[a,c]	1799T>A	Leu160His	N.D.	N.D.	N.D.	N.D.	N.D.	N.D.
*CYP2A6*5*[a,c]	6582G>T	Gly479Val	N.D.	N.D.	N.D.	N.D.	N.D.	N.D.
*CYP2A6*6*[a,c]	1703G>A	Arg128Gln	N.D.	N.D.	N.D.	N.D.	N.D.	N.D.
*CYP2A6*7*	6558T>C	Ile471Thr	267 ± 59.9	2.36 ± 0.41	9.14 ± 2.44* (5%)	4.55 ± 1.94	3.33 ± 0.62	0.80 ± 0.17* (26%)
*CYP2A6*8*	6600G>T	Arg485Leu	103 ± 16.3	2.10 ± 0.24	20.6 ± 2.44* (12%)	3.13 ± 0.30	2.22 ± 0.16*	0.71 ± 0.06*** (23%)
*CYP2A6*10*[b,d]	6558T>C 6600G>T	Ile471Thr Arg485Leu	N.D.	N.D.	N.D.	N.D.	N.D.	N.D.
*CYP2A6*11*	3391T>C	Ser224Pro	142 ± 31.3	4.31 ± 0.34	31.6 ± 5.88* (18%)	3.30 ± 0.37	2.57 ± 0.03*	0.79 ± 0.09*** (26%)
*CYP2A6*13*	13G>A	Gly5Arg	30.8 ± 0.80	3.94 ± 0.20	128 ± 5.36 (73%)	1.37 ± 0.03*	2.61 ± 0.19	1.90 ± 0.17 (63%)
*CYP2A6*14*	86G>A	Ser29Asn	28.8 ± 0.65	7.01 ± 0.12	243 ± 5.67 (138%)	1.77 ± 0.15	8.02 ± 0.43	4.53 ± 0.16* (149%)
*CYP2A6*15*	2134A>G	Lys194Glu	23.4 ± 0.74	9.03 ± 0.09	385 ± 8.46*** (219%)	1.27 ± 0.03*	9.10 ± 0.31*	7.17 ± 0.28* (236%)
*CYP2A6*16*	21611C>A	Arg203Ser	39.0 ± 2.52	4.58 ± 0.26	118 ± 3.60 (67%)	1.93 ± 0.15	4.72 ± 0.14	2.46 ± 0.21 (81%)
*CYP2A6*17*	5065G>A	Val365Met	25.9 ± 6.16	1.70 ± 0.21	68.3 ± 12.2* (39%)	1.72 ± 0.03	2.76 ± 0.08*	1.60 ± 0.02** (53%)
*CYP2A6*18*	5668A>T	Tyr392Phe	82.1 ± 7.42	7.94 ± 0.63	97.1 ± 6.86 (55%)	2.77 ± 0.18	8.03 ± 0.43	2.90 ± 0.05 (95%)
*CYP2A6*19*	5668A>T 6558T>C	Tyr392Phe Ile471Thr	405 ± 118	2.29 ± 0.46	5.80 ± 0.53* (3%)	4.75 ± 0.14***	2.18 ± 0.08*	0.46 ± 0.01*** (15%)
*CYP2A6*21*	6573A>G	Lys476Arg	40.3 ± 3.69	6.15 ± 0.33	153 ± 9.35 (87%)	2.34 ± 0.29	6.20 ± 0.35	2.67 ± 0.20 (88%)
*CYP2A6*22*	1794C>G 1798C>A	Asp158Glu Leu160Ile	53.8 ± 1.70	6.26 ± 0.36	116 ± 6.49 (66%)	2.40 ± 0.10	5.28 ± 0.20	2.20 ± 0.06* (72%)
*CYP2A6*23*	2161C>T	Arg203Cys	41.1 ± 3.50	3.73 ± 0.32	91.1 ± 8.08* (52%)	1.88 ± 0.04	4.86 ± 0.17	2.59 ± 0.04 (85%)
*CYP2A6*24*	594G>A 6458A>T	Val110Leu Asn438Tyr	52.4 ± 8.56	4.79 ± 0.30	93.4 ± 12.1 (53%)	2.22 ± 0.18	3.23 ± 0.11	1.46 ± 0.07*** (48%)
*CYP2A6*25*[d]	1672T>C	Phe118Leu	59.9 ± 5.94	1.67 ± 0.09	28.0 ± 2.48* (16%)	N.D.	N.D.	N.D.
*CYP2A6*26*[a,c]	1672T>C 1703G>T 1711T>G	Phe118Leu Arg128Leu Ser131Ala	N.D.	N.D.	N.D.	N.D.	N.D.	N.D.
*CYP2A6*28*	5745A>G 5750G>C	Asn418Asp Glu419Asp	35.0 ± 4.19	6.30 ± 0.73	181 ± 14.7 (103%)	1.43 ± 0.12	5.05 ± 0.25	3.55 ± 0.23 (117%)
*CYP2A6*31*	16A>C	Met6Leu	35.4 ± 6.15	6.30 ± 0.30	184 ± 36.3 (105%)	1.61 ± 0.07	5.64 ± 0.13	3.50 ± 0.12 (115%)
*CYP2A6*35*	6458A>T	Asn438Tyr	75.7 ± 14.9	3.98 ± 0.51	53.5 ± 5.31* (30%)	2.50 ± 0.28	4.63 ± 0.35	1.86 ± 0.08*** (61%)
*CYP2A6*36*[b,d]	6458A>T 6558T>C	Asn438Tyr Ile471Thr	N.D.	N.D.	N.D.	N.D.	N.D.	N.D.
*CYP2A6*37*[b,c]	6458A>T 6558T>C 6600G>T	Asn438Tyr Ile471Thr Arg485Leu	N.D.	N.D.	N.D.	N.D.	N.D.	N.D.
*CYP2A6*38*	5023T>C	Tyr351His	108 ± 9.63*	2.37 ± 0.12	22.2 ± 2.84* (13%)	1.51 ± 0.08	2.07 ± 0.02*	1.37 ± 0.07*** (45%)
*CYP2A6*39*	468G>A	Val68Met	93.7 ± 20.4	1.91 ± 0.03	21.4 ± 4.72* (12%)	1.50 ± 0.20	1.85 ± 0.02*	1.26 ± 0.16* (41%)
*CYP2A6*40*	1767C>G	Ile149Met	168 ± 72.0	1.97 ± 0.31	13.0 ± 2.93* (7%)	1.34 ± 0.08*	1.33 ± 0.08*	0.99 ± 0.01** (33%)
*CYP2A6*41*	3515G>A	Arg265Gln	263 ± 82.3	2.15 ± 0.43	8.43 ± 0.95* (5%)	2.32 ± 0.23	1.26 ± 0.04*	0.54 ± 0.04*** (18%)
*CYP2A6*42*	3524T>C	Ile268Thr	450 ± 72.9	2.72 ± 0.37	6.07 ± 0.24* (3%)	3.25 ± 0.44	0.63 ± 0.02*	0.20 ± 0.02*** (6%)
*CYP2A6*43*	4406C>T	Thr303Ile	1049 ± 683	4.76 ± 2.00	5.33 ± 1.28* (3%)	8.55 ± 1.47	1.34 ± 0.09*	0.16 ± 0.02*** (5%)
*CYP2A6*44*[d]	5661G>A 5745A>G 5750G>C	Glu390Lys Asn418Asp Glu419Asp	1097 ± 284	2.39 ± 0.43	2.22 ± 0.16* (1%)	N.D.	N.D.	N.D.
*CYP2A6*45*	6531C>T	Leu462Pro	55.1 ± 11.3	1.19 ± 0.12	22.0 ± 2.24* (13%)	1.65 ± 0.16	1.07 ± 0.02*	0.65 ± 0.05*** (21%)

N.D., Not determined.

*$P < 0.05$, **$P < 0.01$, and ***$P < 0.005$ compared with CYP2A6.1.

[a]The kinetic parameters for nicotine *C*-oxidation of CYP2A6.2, CYP2A6.5, CYP2A6.6, and CYP2A6.26 could not be determined because the enzymatic activity of P450 was not detected at the highest substrate concentration (1000 μas not detec

[b]The kinetic parameters for nicotine C-oxidation of CYP2A6.10, CYP2A6.36, and CYP2A6.37 could not be determined because the amount of product, cotinine, produced by these variants was below the quantification limit at low substrate concentrations.

[c]The kinetic parameters of CYP2A6.2, CYP2A6.5, CYP2A6.6, CYP2A6.26, and CYP2A6.37 could not be determined because the enzymatic activity of P450 was not detected at the highest substrate concentration (25 μas not detec

[d]The kinetic parameters for nicotine *C*-oxidation of CYP2A6.10, CYP2A6.25, CYP2A6.36, and CYP2A6.44 could not be determined because the amount of product, 7-hydroxycoumarin, produced by these variants was below the quantification limit at low substrate concentrations.

The kinetic parameters of coumarin 7-hydroxylation were determined for 25 CYP2A6 variants, as shown in Table 1. The K_m, V_{max}, and CL_{int} values for coumarin 7-hydroxylation by the wild-type enzyme were 1.94 μM, 5.89 pmol · min^{-1} · pmol^{-1} CYP2A6, and 3.04 μl · min^{-1} · pmol^{-1} CYP2A6, respectively. The kinetic parameters of CYP2A6.2, CYP2A6.5, CYP2A6.6, CYP2A6.26, and CYP2A6.37 could not be determined because no coumarin 7-hydroxylation activity was detected. The kinetic parameters of four variants (CYP2A6.10, CYP2A6.25, CYP2A6.36, and CYP2A6.44) could not be determined because the amount of 7-hydroxycoumarin product produced by these variants was below the quantification limit at low substrate concentrations. Compared with the K_m value for CYP2A6.1, that for CYP2A6.19 was significantly elevated by 2.4-fold. In contrast, the K_m values of CYP2A6.13, CYP2A6.15, and CYP2A6.40 were significantly reduced. CYP2A6.15 exhibited a V_{max} value that was 1.5-fold higher than that of the wild-type CYP2A6. The V_{max} values of eleven variants (CYP2A6.8, CYP2A6.11, CYP2A6.17, CYP2A6.19, CYP2A6.38, CYP2A6.39, CYP2A6.40, CYP2A6.41, CYP2A6.42, CYP2A6.43, and CYP2A6.45) were significantly lower than that of CYP2A6.1. The CL_{int} values for CYP2A6.14 and CYP2A6.15 were significantly higher than that of the wild type, and those of 13 variants (CYP2A6.7, CYP2A6.8, CYP2A6.11, CYP2A6.17, CYP2A6.19, CYP2A6.22, CYP2A6.24, CYP2A6.35, CYP2A6.40, CYP2A6.41, CYP2A6.42, CYP2A6.43, and CYP2A6.45) were significantly lower than that of the wild type.

After calculating the CL_{int} values for nicotine *C*-oxidation and coumarin 7-hydroxylation, a significant correlation was found between these values among the different variants ($R^2 = 0.970$, $P < 0.001$), as shown in Fig. 3. CYP2A6.2, CYP2A6.5, CYP2A6.6, CYP2A6.10, CYP2A6.26, CYP2A6.36, and CYP2A6.37 were catalytically inactive toward both nicotine and coumarin.

Discussion

CYP2A6 is an important enzyme that metabolizes several tobacco components, including nicotine, NNK, and NNN. CYP2A6 genetic polymorphisms are believed to affect individual variation in smoking behavior and tobacco-related lung cancer risk. In the present study, the effects of 34 CYP2A6 variant alleles on enzyme activity were characterized by overexpressing the variant proteins in 293FT cells. Among the CYP2A6 variants, the kinetic parameters for nicotine *C*-oxidation and coumarin 7-hydroxylation were determined for 27 and 25 variants, respectively. Thus, it is likely that the measured enzymatic properties were affected by the allelic polymorphisms present in each variant.

Our results revealed that there was a significant correlation between the CL_{int} values for nicotine *C*-oxidation and coumarin 7-hydroxylation among CYP2A6 variants. In particular, metabolic activity on both nicotine and coumarin substrates was virtually abolished in CYP2A6.2, CYP2A6.5, CYP2A6.6, CYP2A6.10, CYP2A6.26, CYP2A6.36, and CYP2A6.37. Similarly, the CL_{int} of CYP2A6.10 expressed in Sf9 cells was shown to reduce the metabolism of tegafur to 0.6% of the wild-type CYP2A6 (Yamamiya et al., 2014). Thus, these inactive variant enzymes are predicted to exhibit markedly reduced catalytic metabolism in the presence of other clinical drugs and activation of procarcinogens similar to nicotine and coumarin. Such variants may influence individual differences in drug efficacies, adverse effects, and cancer risks.

The nicotine *C*-oxidation and coumarin 7-hydroxylation activities of CYP2A6.17, CYP2A6.19, CYP2A6.25, CYP2A6.26, CYP2A6.35, CYP2A6.36, CYP2A6.37, and CYP2A6.43 were reduced compared with those of CYP2A6.1. The amino acid substitutions in these variant alleles exists in conserved regions among P450 isoforms and are critical to enzymatic function. *CYP2A6*17*, carrying the Val365Met amino acid substitution, was found in African-American subjects with a frequency of 9.4% (Fukami et al., 2004).

The substituted residue is located in substrate-recognition site (SRS)-5, some amino acid chains of which form the heme pocket. *CYP2A6*25* and *CYP2A6*26* were identified in an African population and include the Phe118Leu substitution (Mwenifumbo et al., 2008). The nicotine metabolic activities for these variants were reduced to 90% when expressed in *Escherichia coli* cells (*CYP2A6*25*) and to 0% (*CYP2A6*26*) for the wild-type. Phe118 is situated in SRS-1 and is predicted to be involved in substrate stability. Moreover, *CYP2A6*26* contains the Arg128Leu substitution, which is thought to be related to holoprotein formation. *CYP2A6*35, CYP2A6*36,* and *CYP2A6*37* were also discovered in an African population (Mwenifumbo et al., 2008; Al Koudsi et al., 2009). These variant alleles include Asn438Tyr, caused by the 6458A>T mutation. Asn438 is located in a heme binding site, suggesting the possibility that the amino acid substitution alters the binding stability of heme. *CYP2A6*43* (4406C>T, Thr303Ile) was identified in African Americans, and its catalytic efficiency was reported to be reduced compared with that of CYP2A6.1 (Piliguian et al., 2014).

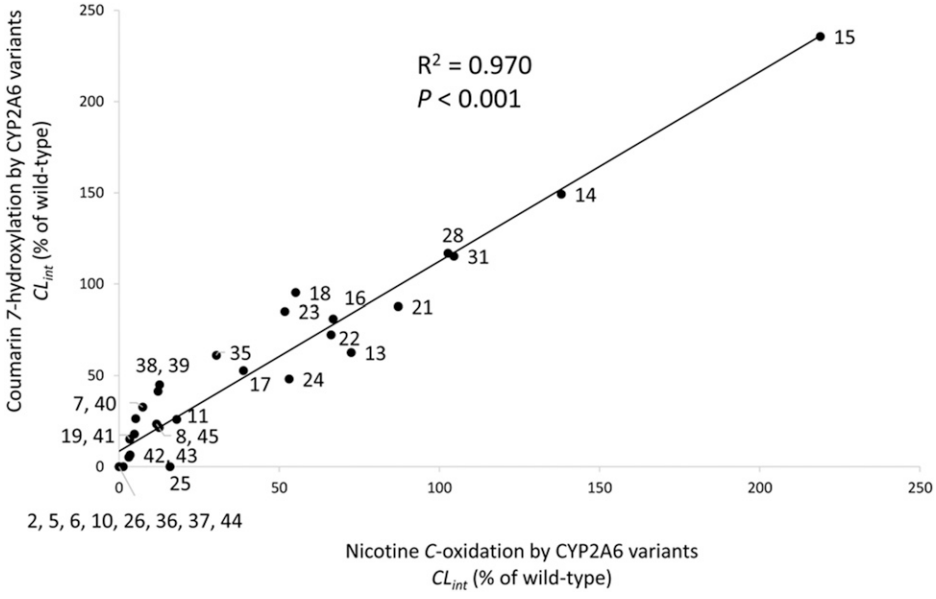

Fig. 3. Correlation between the CL_{int} ratios (relative to the wild type CYP2A6.1) for nicotine *C*-oxidation and coumarin 7-hydroxylation among CYP2A6 variants. Nicotine *C*-oxidation CL_{int} ratios are plotted on the horizontal axis and coumarin 7-hydroxylation CL_{int} ratios are plotted on the vertical axis. Numbers correspond to CYP2A6 variants. Correlation was analyzed using weighted linear regression analysis with IBM SPSS Statistics.

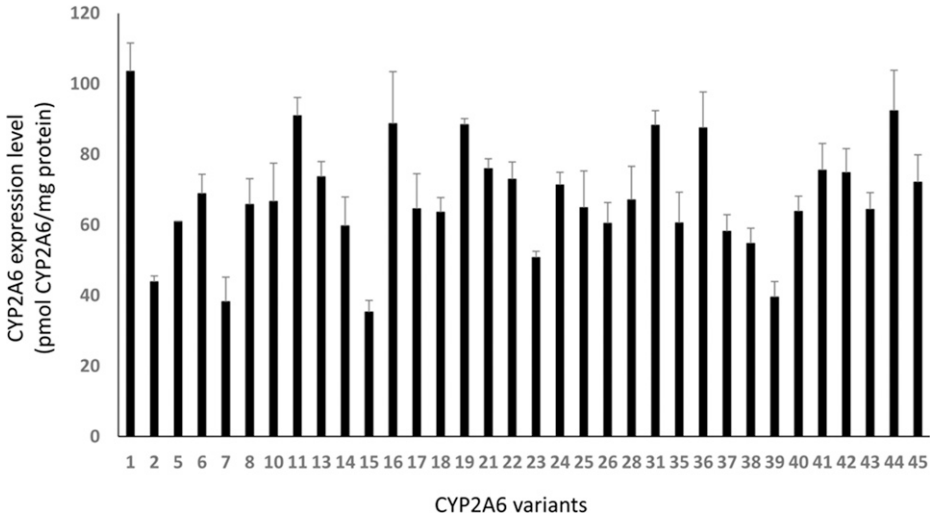

Fig. 4. Average levels of CYP2A6 proteins expressed in 293FT cells. Each bar is presented as the mean ± S.D. of three independently performed immunoblottings. Numbers correspond to CYP2A6 variants.

Thr303 is positioned in SRS-4, and its substitution may negatively impact function and stability. Thus, these mutations in highly conserved P450 regions may affect enzyme activity by altering the stability of the enzyme and/or its affinity to substrates and heme. However, the quantitative protein expression levels differ between CYP2A6 variants owing to alterations in protein stability caused by amino acid replacement variations (Fig. 4). However, it is the limitation of this study that the transfection efficiency for expressing CYP2A6 protein was not evaluated.

The *CYP2A6*7* allele contains a 6558T>C nucleotide substitution causing the Ile471Thr substitution in the β4(1) strand near SRS-6; this substitution is known to decrease the catalytic activity of the enzyme (Ariyoshi et al., 2001; Uno et al., 2013). This amino acid may be involved in determining the conformation of SRS-6. In our study, CYP2A6.8, including the Arg485Leu substitution, exhibited reduced enzymatic activity. This substitution also occurs near SRS-6 and may alter the folding of SRS-6 (Ariyoshi et al., 2001). Both of the above amino acid changes are also included in several other variant alleles (*CYP2A6*10, CYP2A6*19, CYP2A6*36,* and *CYP2A6*37*) and probably affect the enzymatic activities for these alleles as well. For *CYP2A6*13*, two protein bands were detected by immunoblotting. The Gly5Arg amino acid substitution in CYP2A6.13, occurring in the membrane anchor region, may alter the protein's digestion by proteases, thus explaining the additional band. Further studies are needed to confirm these findings.

The 1703G>A single-point mutation in *CYP2A6*6* leads to the Arg128Gln substitution, which is present in the Japanese population with a frequency of 0.4% (Kitagawa et al., 2001). The Arg128 residue is located in a highly conserved region of the P450 superfamily and results in a reduced-CO difference spectrum for hemin-fortified CYP2A6.6 compared with that of the wild-type enzyme. In the 3D structure model of the human CYP2A6, this residue forms hydrogen bonds with Asn438, which is located next to the heme-binding Cys439 (Fig. 5). By eliminating this hydrogen bond, the Arg128Gln substitution may affect the binding of heme and disorder the holoprotein structure. The *CYP2A6*11* allele (3391T>C, Ser224Pro) was identified in a Japanese patient exhibiting a high plasma tegafur concentration-time curve (Daigo et al., 2002). According to our analysis, the coumarin 7-hydroxylation activity of CYP2A6.11 was significantly reduced by 26% compared with that of CYP2A6.1. Although Ser224 is not located in a highly conserved region, this amino acid forms a hydrogen bond with Tyr220 and contributes to the folding of an α-helix. The Ser224Pro substitution may abrogate the hydrogen bond and alter the 3D structure of the CYP2A6 enzyme. The single-nucleotide polymorphism in *CYP2A6*15* results in the Lys194Glu substitution and significantly higher metabolic activity with both substrates. Although Lys194 is not located within a highly conserved region, the substitution is considered to be indirectly adjacent to the F-helix and SRS-2 (Uno et al., 2013). CYP2A6.44 was also found to exhibit markedly reduced enzymatic activity in the presence of both substrates. *CYP2A6*44* was identified in an African American and contains the Glu390Lys amino acid substitution (Piliguian et al., 2014). Glu390 is positioned in a β-sheet and forms hydrogen bonds with Glu103 in SRS-1 and Arg76. *CYP2A6*44* alleles may affect the protein conformation of SRS-1, resulting in reduced affinity to CYP2A6 substrates.

In conclusion, we expressed 34 CYP2A6 protein variants in 293FT cell and determined their metabolic activities in vitro. Our results demonstrated the presence of functional variability in enzyme activities

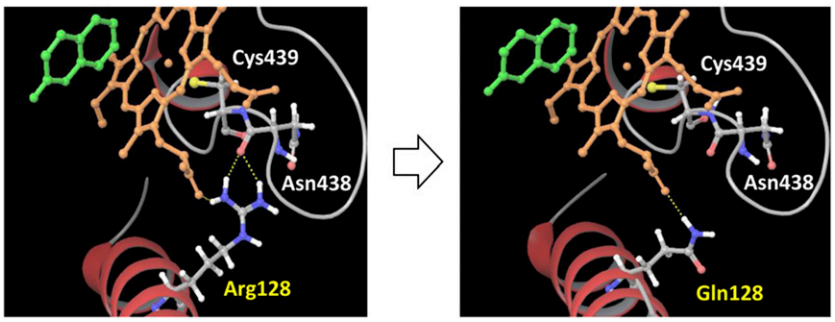

Fig. 5. Diagram of a portion of the CYP2A6 crystal structure showing the Arg128Gln substitution in CYP2A6.6. Ionic bonding differs between the wild-type enzyme and the CYP2A6.6 variant.

resulting from amino acid substitutions caused by genetic polymorphisms. CYP2A6 is an important P450 isoform involved in the metabolism of nicotine, many clinical drugs, and the activation of procarcinogens. These findings provide further insight into individual differences in smoking behaviors, drug efficacies, and cancer susceptibilities.

Acknowledgments

The authors thank the Biomedical Research Core of Tohoku University Graduate School of Medicine for technical support.

Authorship Contributions

Participated in research design: Hosono, Kumondai, Hiratsuka.

Conducted experiments: Hosono, Kumondai.

Contributed new reagents or analytic tools: Maekawa, Yamaguchi, Mano, Hirasawa, Hiratsuka.

Performed data analysis: Hosono, Kumondai, Maekawa, Oda, Hiratsuka.

Wrote or contributed to the writing of the manuscript: Hosono, Kumondai, Hiratsuka.

References

Al Koudsi N, Ahluwalia JS, Lin SK, Sellers EM, and Tyndale RF (2009) A novel CYP2A6 allele (CYP2A6*35) resulting in an amino-acid substitution (Asn438Tyr) is associated with lower CYP2A6 activity in vivo. *Pharmacogenomics J* **9**:274–282.

Ariyoshi N, Sawamura Y, and Kamataki T (2001) A novel single nucleotide polymorphism altering stability and activity of CYP2a6. *Biochem Biophys Res Commun* **281**:810–814.

Benowitz NL, Jacob P, 3rd, and Sachs DP (1995) Deficient C-oxidation of nicotine. *Clin Pharmacol Ther* **57**:590–594.

Crespi CL, Penman BW, Gelboin HV, and Gonzalez FJ (1991) A tobacco smoke-derived nitrosamine, 4-(methylnitrosamino)-1-(3-pyridyl)-1-butanone, is activated by multiple human cytochrome P450s including the polymorphic human cytochrome P4502D6. *Carcinogenesis* **12**:1197–1201.

Daigo S, Takahashi Y, Fujieda M, Ariyoshi N, Yamazaki H, Koizumi W, Tanabe S, Saigenji K, Nagayama S, Ikeda K, et al. (2002) A novel mutant allele of the CYP2A6 gene (CYP2A6*11) found in a cancer patient who showed poor metabolic phenotype towards tegafur. *Pharmacogenetics* **12**:299–306.

DeVore NM and Scott EE (2012) Nicotine and 4-(methylnitrosamino)-1-(3-pyridyl)-1-butanone binding and access channel in human cytochrome P450 2A6 and 2A13 enzymes. *J Biol Chem* **287**:26576–26585.

Fagerström K and Balfour DJ (2006) Neuropharmacology and potential efficacy of new treatments for tobacco dependence. *Expert Opin Investig Drugs* **15**:107–116.

Fernandez-Salguero P, Hoffman SMG, Cholerton S, Mohrenweiser H, Raunio H, Rautio A, Pelkonen O, Huang JD, Evans WE, Idle JR, et al. (1995) A genetic polymorphism in coumarin 7-hydroxylation: sequence of the human CYP2A genes and identification of variant CYP2A6 alleles. *Am J Hum Genet* **57**:651–660.

Fujieda M, Yamazaki H, Saito T, Kiyotani K, Gyamfi MA, Sakurai M, Dosaka-Akita H, Sawamura Y, Yokota J, Kunitoh H, et al. (2004) Evaluation of CYP2A6 genetic polymorphisms as determinants of smoking behavior and tobacco-related lung cancer risk in male Japanese smokers. *Carcinogenesis* **25**:2451–2458.

Fukami T, Nakajima M, Yoshida R, Tsuchiya Y, Fujiki Y, Katoh M, McLeod HL, and Yokoi T (2004) A novel polymorphism of human CYP2A6 gene CYP2A6*17 has an amino acid substitution (V365M) that decreases enzymatic activity in vitro and in vivo. *Clin Pharmacol Ther* **76**:519–527.

Haberl M, Anwald B, Klein K, Weil R, Fuss C, Gepdiremen A, Zanger UM, Meyer UA, and Wojnowski L (2005) Three haplotypes associated with CYP2A6 phenotypes in Caucasians. *Pharmacogenet Genomics* **15**:609–624.

Han S, Choi S, Chun YJ, Yun CH, Lee CH, Shin HJ, Na HS, Chung MW, and Kim D (2012) Functional characterization of allelic variants of polymorphic human cytochrome P450 2A6 (CYP2A6*5, *7, *8, *18, *19, and *35). *Biol Pharm Bull* **35**:394–399.

Hiratsuka M (2012) In vitro assessment of the allelic variants of cytochrome P450. *Drug Metab Pharmacokinet* **27**:68–84.

Ho MK, Mwenifumbo JC, Zhao B, Gillam EM, and Tyndale RF (2008) A novel CYP2A6 allele, CYP2A6*23, impairs enzyme function in vitro and in vivo and decreases smoking in a population of Black-African descent. *Pharmacogenet Genomics* **18**:67–75.

Hosono H, Kumondai M, Arai T, Sugimura H, Sasaki T, Hirasawa N, and Hiratsuka M (2015) CYP2A6 genetic polymorphism is associated with decreased susceptibility to squamous cell lung cancer in Japanese smokers. *Drug Metab Pharmacokinet* **30**:263–268.

Kharasch ED, Hankins DC, and Thummel KE (1995) Human kidney methoxyflurane and sevoflurane metabolism. Intrarenal fluoride production as a possible mechanism of methoxyflurane nephrotoxicity. *Anesthesiology* **82**:689–699.

Kitagawa K, Kunugita N, Kitagawa M, and Kawamoto T (2001) CYP2A6*6, a novel polymorphism in cytochrome p450 2A6, has a single amino acid substitution (R128Q) that inactivates enzymatic activity. *J Biol Chem* **276**:17830–17835.

Kiyotani K, Fujieda M, Yamazaki H, Shimada T, Guengerich FP, Parkinson A, Nakagawa K, Ishizaki T, and Kamataki T (2002) Twenty one novel single nucleotide polymorphisms (SNPs) of the CYP2A6 gene in Japanese and Caucasians. *Drug Metab Pharmacokinet* **17**:482–487.

Komatsu T, Yamazaki H, Shimada N, Nakajima M, and Yokoi T (2000) Roles of cytochromes P450 1A2, 2A6, and 2C8 in 5-fluorouracil formation from tegafur, an anticancer prodrug, in human liver microsomes. *Drug Metab Dispos* **28**:1457–1463.

Kumondai M, Hosono H, Orikasa K, Arai Y, Arai T, Sugimura H, Ozono S, Sugiyama T, Takayama T, Sasaki T, et al. (2016) Genetic polymorphisms of CYP2A6 in a case-control study on bladder cancer in Japanese smokers. *Biol Pharm Bull* **39**:84–89.

Loukola A, Buchwald J, Gupta R, Palviainen T, Hällfors J, Tikkanen E, Korhonen T, Ollikainen M, Sarin AP, Ripatti S, et al. (2015) A genome-wide association study of a biomarker of nicotine metabolism. *PLoS Genet* **11**:e1005498.

Miles JS, McLaren AW, Forrester LM, Glancey MJ, Lang MA, and Wolf CR (1990) Identification of the human liver cytochrome P-450 responsible for coumarin 7-hydroxylase activity. *Biochem J* **267**:365–371.

Mwenifumbo JC, Al Koudsi N, Ho MK, Zhou Q, Hoffmann EB, Sellers EM, and Tyndale RF (2008) Novel and established CYP2A6 alleles impair in vivo nicotine metabolism in a population of Black African descent. *Hum Mutat* **29**:679–688.

Nakajima M, Fukami T, Yamanaka H, Higashi E, Sakai H, Yoshida R, Kwon JT, McLeod HL, and Yokoi T (2006) Comprehensive evaluation of variability in nicotine metabolism and CYP2A6 polymorphic alleles in four ethnic populations. *Clin Pharmacol Ther* **80**:282–297.

Nakajima M, Yamamoto T, Nunoya K, Yokoi T, Nagashima K, Inoue K, Funae Y, Shimada N, Kamataki T, and Kuroiwa Y (1996) Role of human cytochrome P4502A6 in C-oxidation of nicotine. *Drug Metab Dispos* **24**:1212–1217.

Oldham RK (1998) Principles of Cancer Biotherapy, 3rd ed., Springer Science+Business Media LLC, New York, pp 51–77.

Oscarson M, McLellan RA, Gullstén H, Agúndez JA, Benítez J, Rautio A, Raunio H, Pelkonen O, and Ingelman-Sundberg M (1999) Identification and characterisation of novel polymorphisms in the CYP2A locus: implications for nicotine metabolism. *FEBS Lett* **460**:321–327.

Pan L, Yang X, Li S, and Jia C (2015) Association of CYP2A6 gene polymorphisms with cigarette consumption: a meta-analysis. *Drug Alcohol Depend* **149**:268–271.

Patel YM, Park SL, Han Y, Wilkens LR, Bickeböller H, Rosenberger A, Caporaso N, Landi MT, Brüske I, Risch A, et al. (2016) Novel association of genetic markers affecting CYP2A6 activity and lung cancer risk. *Cancer Res* **76**:5768–5776.

Pearce RE, Cohen-Wolkowiez M, Sampson MR, and Kearns GL (2013) The role of human cytochrome P450 enzymes in the formation of 2-hydroxymetronidazole: CYP2A6 is the high affinity (low Km) catalyst. *Drug Metab Dispos* **41**:1686–1694.

Pelkonen O, Rautio A, Raunio H, and Pasanen M (2000) CYP2A6: a human coumarin 7-hydroxylase. *Toxicology* **144**:139–147.

Piliguian M, Zhu AZ, Zhou Q, Benowitz NL, Ahluwalia JS, Sanderson Cox L, and Tyndale RF (2014) Novel CYP2A6 variants identified in African Americans are associated with slow nicotine metabolism in vitro and in vivo. *Pharmacogenet Genomics* **24**:118–128.

Sadeque AJ, Fisher MB, Korzekwa KR, Gonzalez FJ, and Rettie AE (1997) Human CYP2C9 and CYP2A6 mediate formation of the hepatotoxin 4-ene-valproic acid. *J Pharmacol Exp Ther* **283**:698–703.

Soriano A, Vicente J, Carcas C, Gonzalez-Andrade F, Arenaz I, Martinez-Jarreta B, Fanlo A, Mayayo E, and Sinués B (2011) Differences between Spaniards and Ecuadorians in CYP2A6 allele frequencies: comparison with other populations. *Fundam Clin Pharmacol* **25**:627–632.

Uno T, Obe Y, Ogura C, Goto T, Yamamoto K, Nakamura M, Kanamaru K, Yamagata H, and Imaishi H (2013) Metabolism of 7-ethoxycoumarin, safrole, flavanone and hydroxyflavanone by cytochrome P450 2A6 variants. *Biopharm Drug Dispos* **34**:87–97.

Wang H, Bian T, Liu D, Jin T, Chen Y, Lin A, and Chen C (2011) Association analysis of CYP2A6 genotypes and haplotypes with 5-fluorouracil formation from tegafur in human liver microsomes. *Pharmacogenomics* **12**:481–492.

Yamamiya I, Yoshisue K, Ishii Y, Yamada H, and Chiba M (2014) Effect of CYP2A6 genetic polymorphism on the metabolic conversion of tegafur to 5-fluorouracil and its enantioselectivity. *Drug Metab Dispos* **42**:1485–1492.

Yano JK, Hsu MH, Griffin KJ, Stout CD, and Johnson EF (2005) Structures of human microsomal cytochrome P450 2A6 complexed with coumarin and methoxsalen. *Nat Struct Mol Biol* **12**:822–823.

Address correspondence to: Dr. Masahiro Hiratsuka, Laboratory of Pharmacotherapy of Life-Style–Related Diseases, Graduate School of Pharmaceutical Sciences, Tohoku University, 6-3 Aoba, Aramaki, Aoba-ku, Sendai 980-8578, Japan. E-mail: mhira@m.tohoku.ac.jp